The long road

Hilgendorf, Susan


4

Inhibition of autophagy as treatment strategy for p53 wild type acute myeloid leukemia

Hendrik Folkerts[1], Susan Hilgendorf[1], Albertus T.J. Wierenga[1,2], Jennifer Jaques[1] , André B. Mulder[2], Paul J. Coffer[3,4], Jan Jacob Schuringa[1], Edo Vellenga[1]

[1] Department of Experimental Hematology, Cancer Research Center Groningen, University Medical Center Groningen, University of Groningen, Groningen, the Netherlands

[2] Department of Laboratory Medicine, University Medical Center Groningen, Groningen, the Netherlands.

[3] Regenerative Medicine Center, University Medical Center Utrecht, Utrecht, the Netherlands

[4] Center of Molecular Medicine, University Medical Center Utrecht, the Netherlands

Adapted from Cell Death & Disease 2017;8:2927

ABSTRACT

Here we have explored whether inhibition of autophagy can be used as treatment strategy for acute myeloid leukemia (AML). Steady-state autophagy was measured in leukemic cell lines and primary human $CD34^+$ AML cells with a large variability in basal autophagy between AMLs observed. The autophagy-flux was higher in AMLs classified as poor-risk, which are frequently associated with TP53 mutations ($TP53^{mut}$), compared to favorable- and intermediate-risk AMLs. In addition, the higher flux was associated with a higher expression level of several autophagy genes, but was not affected by alterations in p53 expression by knocking down p53 or overexpression of wild type p53 or $p53^{R273H}$. AML $CD34^+$ cells were more sensitive to the autophagy inhibitor hydroxychloroquine (HCQ) than normal bone marrow $CD34^+$ cells. Similar, inhibition of autophagy by knockdown of ATG5 or ATG7 triggered apoptosis, which coincided with increased expression of p53. In contrast to wild type p53 AML ($TP53^{wt}$), HCQ treatment did not trigger a BAX and PUMA-dependent apoptotic response in AMLs harboring $TP53^{mut}$. To further characterize autophagy in the leukemic stem cell (LSC)-enriched cell fraction AML $CD34^+$ cells were separated into ROS^{low} and ROS^{high} subfractions. The immature AML-$CD34^+$-enriched ROS^{low} cells maintained higher basal autophagy and showed reduced survival upon HCQ treatment compared to ROS^{high} cells. Finally, knockdown of ATG5 inhibits *in vivo* maintenance of AML $CD34^+$ cells in NSG mice. These results indicate that targeting autophagy might provide new therapeutic options for treatment of AML since it affects the immature AML subfraction.

INTRODUCTION

AML is characterized by the accumulation of immature blast cells in the bone marrow, resulting in a disruption of normal hematopoiesis. The growth advantage of leukemic cells over the normal hematopoietic stem and progenitor cells (HPSC) is linked to a perturbation in differentiation, metabolic and cell survival programming, as result of a number of genetic and epigenetic defects.[1-3] Transcriptome studies have demonstrated that the expression patterns of apoptotic and anti-apoptotic genes are significantly different between AML $CD34^+$ cells compared to $CD34^+$ cells derived from healthy subjects.[4, 5]

HPSC homeostasis requires macroautophagy (here referred to as autophagy), which is an alternative cell survival program involved in degradation of redundant organelles and proteins.[6-8] Autophagic flux in normal HSPC is most prominent in the immature $CD34^+CD38^-$ subfraction and declines in more differentiated myeloid cells.[9] Maintenance of an adequate level of autophagy is essential for HPSC homeostasis. Previous studies have shown that lentiviral knockdown of the essential autophagy genes ATG5 and ATG7 results in impaired engraftment of cord blood (CB) $CD34^+$ cells in NSG mice.[9, 10] In addition, $ATG7^{null}$ or $ATG5^{null}$ mice develop anemia and during long-term follow-up myelodysplasia.[11-13] Recent studies in myeloid leukemia have suggested that in AML the autophagy machinery might be disrupted, resulting in intracellular accumulation of damaged mitochondria and increased levels of reactive oxygen species (ROS); with high ROS levels potentially promoting leukemic transformation.[12, 14-15] In contrast, other studies have shown that leukemic cells require functional autophagy during leukemia maintenance.[16-18] In addition, autophagy can be an escape mechanism utilized by leukemic cells after treatment with chemotherapeutics such as mTOR- and HDAC inhibitors [19-25] Together, this suggests a greater dependency of AML cells on these effector pathways. The aim of our study was to determine whether inhibiting autophagy can provide an additional means to impair LSC functionality. We demonstrated that AML $CD34^+$ cells are more susceptible for autophagy inhibition than normal $CD34^+$ cells. P53 is an important effector pathway in the observed apoptotic responds, triggered by inhibition of autophagy.

MATERIAL AND METHODS

Isolation and culture of human $CD34^+$ cells

We obtained umbilical cord blood (UCB) from full-term healthy neonates who were born at the Obstetrics departments of the Martini Hospital and the University Medical Center Groningen (Groningen, the Netherlands). Informed consent was obtained to use UCBs and patients AML blasts derived from peripheral blood cells or bone marrow in accordance with

the Declaration of Helsinki; the protocols were approved by the Medical Ethics Committee of the University Medical Center Groningen (UMCG). Mononuclear cells (MNC) were isolated from UCB, or peripheral blood or bone marrow from AML patients by Ficol density centrifugation, and $CD34^+$ cells were subsequently isolated with the autoMACS pro-separator (Miltenyi Biotec, Amsterdam, the Netherlands).

Cell culture

Primary AML, normal bone marrow or CB-derived $CD34^+$ cells were cultured in suspension or in T25 flasks pre-coated with MS5 stromal cells in Gartners medium: Alpha-MEM (Lonza, Leusden, the Netherlands) supplemented with 12.5% FCS and 12.5% Horse serum (Sigma-Aldrich, Saint Louis, USA), 1% penicillin/streptomycin (PAA Laboratories, Dartmouth, USA), 1 μM hydrocortisone (Sigma-Aldrich), 57.2 mM β–mercaptoethanol and cytokines: G-CSF, Human TPO agonist; Romiplostim (Amgen, Breda, the Netherlands) and IL-3 (20 ng/mL each).[26] For the autophagic-flux AML $CD34^+$ cells were cultured for 3 days on a MS5 stromal layer. Subsequently, the autophagic-flux was determined with cyto-ID. The relative increase in Cyto-ID signal after overnight incubation with 20 μM hydroxychloroquine (HCQ) is considered to be the autophagy flux.[9] The used concentration and incubation time of HCQ for measuring autophagic-flux was validated and is based on maximal accumulation of autophagosomes, without affecting cell viability after overnight incubation with HCQ. AMLs that did not expand were excluded from analysis. The leukemic cell lines HL60, K562, THP1, OCIM3, MOLM13, and NB4 cells were cultured in RPMI 1640, supplemented with 10% FCS and 1% penicillin/streptomycin. KG1A cells were cultured in IMDM (Lonza, Leusden, the Netherlands) 20% FCS and 1% penicillin/streptomycin.

Flowcytometry analysis

After isolation, cells were resuspended in PBS and subsequently incubated for 30 min at 4°C with anti-human CD19, CD34, CD38, CD33 and CD45. After incubation, cells were washed and optionally incubated for 30 min at 37˚C using Cyto-ID Autophagy Detection dye (ENZ-51031-0050, Enzo Life Sciences, Raamsdonksveer, The Netherlands). The cells were subsequently washed and analyzed by flow cytometric analysis (FACS). (Additional information can be found in Supplementary Table S5). All data was analyzed using FlowJo (Tree Star, Oregon, USA) software.

Apoptosis, ROS and mitochondrial mass measurements

Apoptosis was quantified by staining with APC-conjugated Annexin-V (Beckton Dickinson, Franklin Lakes, USA) according to manufacturer's protocol. Reactive oxygen species (ROS) analyses were performed by means of CellROX deep red (APC) or CellROX green (FITC, Life Technologies, Landsmeer, the Netherlands), according to manufacturer's protocol.

Mitochondrial mass was determined with Mitotracker staining (Life Technologies), according to manufacturer's protocol. Apoptosis, CellROX and mitochondrial mass were analyzed by FACS.

Virus production and transduction of CD34$^+$ leukemic cells

shATG7 (TRCN0000007586, Sigma-Aldrich) and shATG5 (TRCN0000151474, Sigma-Aldrich) and shP53 vectors were cloned and extensively validated, as previously described.[9] An shRNA sequence that does not target human genes (referred to as scrambled) was used as a control. TP53^{R273H} or TP53^{wt} were generated by PCR amplification from cDNA obtained from MDA-MB-468 or MOLM13 cells, respectively. Amplified cDNA was subsequently cloned into pRRL-IRES-mBlueberry vector[27], using EcoR1 restriction sites. Lentiviral virions were produced by transient transfection of HEK 293T cells with pCMV and VSV-G packing system using Polyethylenimine (Polyscience Inc. Eppelheim, Germany) or FuGENE (Promega, Leiden, the Netherlands). Retroviral virions containing pBABE-puro-mCherry-EGFP-LC3B (kind gift from Prof. Andrew Thorburn, Dept. of Pharmacology, University of Colorado Cancer Center) were produced by transient transfection of HEK 293T cells with VSV-G, pAmpho packing system and FuGENE. Viral supernatants were collected and filtered through a 0.2-µm filter and subsequently concentrated using Centriprep Ultracel YM-50 centrifugal filters (Millipore). 0.5×10^6 CD34$^+$ cells were seeded in Gartners medium supplemented with cytokines (specified previously). Transduction was performed by adding 0.5 mL of ~10 times concentrated viral supernatant to 0.5 mL of medium in the presence of 4 µg/mL polybrene (Sigma-Aldrich). For retroviral transfections, cells were transfected in retronectin-coated 24-well plates.

Quantitative real-time PCR

Quantitative RT-PCR was used to analyze the mRNA levels of ATG5, Beclin1, ATG8/LC3, VMP1, ATG10, ATG7, BAX, PUMA, BCL-2 PHLDA3, p21, p53, FOXO3A, SOD1, SOD2 and Catalase. Total RNA was isolated from at least $1x10^5$ cells using the RNeasy kit (Qiagen, Venlo, the Netherlands). RNA was reverse transcribed with iScript reverse Transcription kit (Biorad, Veenendaal, the Netherlands). The cDNA obtained was real-time amplified, in iQ SYBR Green Supermix (Bio-Rad), with the CFX connect Thermocycler (Bio-Rad). RPL27 and RPS11 were used as housekeeping genes. The primer sequences are listed in the Supplemental Table S6.

In vivo transplantation of AML CD34$^+$ cells into NSG mice

For transplantation, 12-13 week-old female NSG (NOD.Cg-Prkdcscid IL2rgtm1Wjl/SzJ) mice were purchased from the Central Animal Facility breeding facility at the UMCG. Mouse experiments were performed in accordance with national and institutional guidelines, and

all experiments were approved by the Institutional Animal Care and Use Committee of the University of Groningen (IACUC-RuG). General aspects of these experiments have been described previously[9, 28], and the detailed experimental approach is described in the Supplementary Methods.

Statistical analysis

An unpaired two-sided student's test was used to calculate statistical differences. A P-value of <0.05 was considered statistically significant.

RESULTS

Leukemic cell lines with an increased autophagic flux are more dependent on autophagy for their survival.

During autophagy double membrane vesicles called autophagosomes are formed, which fuse with lysosomes.[6] It is important not only to measure the steady-state number of autophagosomes, but also the turnover.[29] This can be done by staining cells with Cyto-ID, a dye that selectively labels autophagic vacuoles. The relative increase in Cyto-ID signal after overnight incubation with hydroxychloroquine (HCQ) is considered to be the autophagy flux.[9] In the tested cell lines autophagy flux varied, HL60 cells had a significantly lower flux as compared to OCIM3, MOLM13, KG1A and NB4 cells (**Fig 1A-B**; Supplementary Table S1). These results were confirmed by using alternative methods for analyzing autophagy flux. First, cell lines expressing GFP-ATG8/LC3 were treated with or without the autophagy inhibitor Bafilomycin-1A (BAF). The relative accumulation of GFP-ATG8/LC3 puncta upon BAF treatment is indicative for the level of autophagy flux (S1A). Representative pictures of GFP-ATG8/LC3 puncta accumulation in NB4 cells are depicted in S1B**.** In addition, autophagic flux was determined by tandem fluorescent tagged LC3 reporter (**Fig 1C**) and relative accumulation of LC3-II by Western blotting **(Fig 1D,** S1C-D). To confirm that the observed autophagic flux measurements in combination with HCQ were autophagy specific, HL60 and NB4 cells were pre-treated with 5 mM 3-Methyladenine (PI3K inhibitor) or 10 μM SBI-0206965 (ULK1 inhibitor), thereby blocking autophagosome formation. By inhibiting PI3K or ULK1 a near complete block in HCQ dependent LC3-II accumulation was observed underscoring an autophagy specific mechanism (S1E-F).

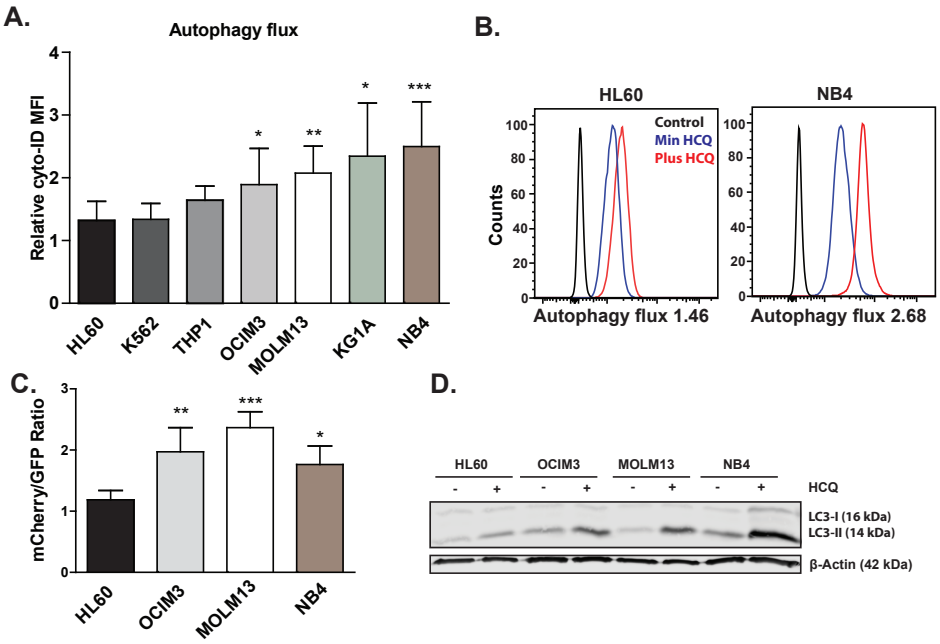

Figure 1. Variation in autophagy flux between different leukemic cell lines. (**A**) Relative accumulation of autophagosomes after overnight treatment with 20 μM HCQ measured by staining with Cyto-ID in a panel of leukemic cell lines (N=7). (**B**) Representative FACS plots showing mean fluorescent intensity of Cyto-ID, with or without HCQ treatment. (**C**) mCherry/GFP ratio in a panel of leukemic cell lines transduced with mCherry-GFP-LC3. (**D**) Representative Western blot of LC3-II accumulation after HCQ in cell lines, β-actin was used as loading control.
Error bars represent SD; *, ** or *** represents p<.05, p<.01 or p<.001, respectively.

To validate whether the observed autophagic flux was functionally relevant, the HL60, MOLM13, OCIM3 and NB4 cell lines were transduced with lentiviral shRNAs, to knockdown the essential autophagy genes ATG5 (shATG5) or ATG7 (shATG7). Each shRNA was selected from a set of 5 individual shRNAs, which were extensively tested as described previously.[9] The knockdown efficiency for shATG5 and shATG7 transduced leukemic cell lines was confirmed by q-PCR (S2A). Lentiviral-mediated knockdown of ATG5 and ATG7 resulted in a reduced accumulation of GFP-ATG8/LC3 puncta after BAF treatment (S2B), which coincided with a significant reduction in survival (**Fig 2A**). To validate these findings in an alternative manner, the cell lines were exposed to different concentrations of HCQ during prolonged culture. Survival and expansion after treatment with HCQ was compared to CB $CD34^+$ cells. CB $CD34^+$ cells showed no impairment in expansion when treated with 5 μM HCQ, while 20 μM HCQ significantly inhibited their expansion (**Fig 2B** and S2C). The cell lines showed variability in survival after HCQ treatment; notably those most susceptible

for HCQ had the highest level of autophagic flux (**Fig 1, Fig 2B** and S2C). The reduced survival and proliferation after inhibition of autophagy was at least in part due to increased apoptosis, as determined by Annexin-V staining (**Fig 2C** and S2D). In MOLM13 and NB4 cells increased apoptosis correlated with increased expression of p53 and its transcriptional target genes BAX, PUMA, and PHLDA3 (S2E).

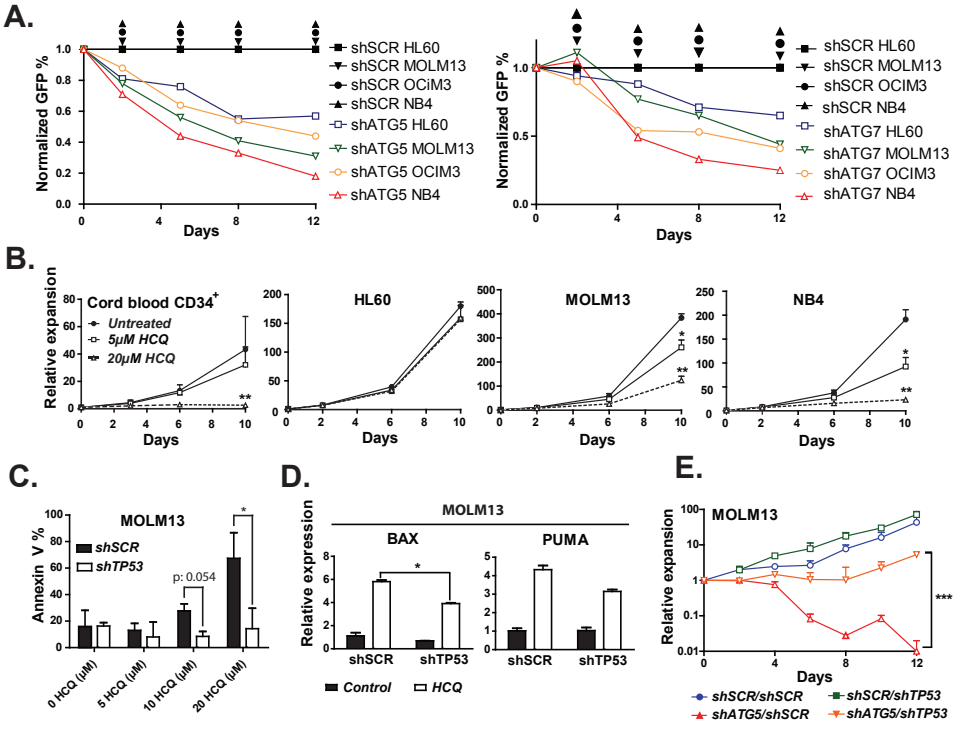

Figure 2. Sensitivity for inhibition of autophagy in leukemic cells. (**A**) Normalized GFP percentages in leukemic cell lines transduced with shSCR-GFP, shATG5-GFP or shATG7-GFP and cultured for 12 days. (**B**) Cumulative growth of leukemia cell lines and cord blood-derived CD34+ cells cultured for 10 days in the presence of 0, 5 or 20 μM HCQ. (**C**) Percentage of Annexin V positive cells in shSCR or shp53 transduced MOLM13 cells, at day 4 after treatment with different concentrations of HCQ. (**D**) Quantitative RT-PCR for BAX and PUMA in shSCR and shP53 transduced MOLM13 cells, treated with 20 μM HCQ for 4 days. (**E**) Cell expansion in time of MOLM13 cells double transduced with shp53-GFP or shSCR-GFP in combination with shSCR-mCherry or shATG5-mCherry. The transduced cells were cultured for 12 days.
Error bars represent SD; *, ** or *** represents p<.05, p<.01 or p<.001, respectively.

To investigate the potential role of p53 in the HCQ-induced cell death, MOLM13 and NB4 were transduced with a lentiviral shRNAs, targeting TP53 (shp53, S2A). The p53 status of used leukemic cell lines is indicated in Supplementary Table S1. Compared to shSCR transduced cells, shp53 transduced cells did not show an apoptotic response to treatment with different HCQ concentrations (**Fig 2C** and S2F). Moreover, knockdown of p53 prevented HCQ-dependent expression of pro-apoptotic BAX and PUMA (**Fig 2D** and S2G)**.** In contrast, $TP53^{null}$ HL60 cells, with low basal autophagy (**Fig 1A**), did not display induction of apoptosis (data not shown) or a strong reduction of expansion upon HCQ treatment (**Fig 2B).** Finally, $p53^{wt}$ cell lines MOLM13 and OCIM3 were double transduced with shSCR- or shP53-GFP in combination with shSCR- or shATG5-mCherry. As expected, knockdown of ATG5 provided a strong reduction in expansion, which could be rescued by additional knockdown of p53. However, following longer follow-up the rescue by shp53 gradually declined (**Fig 2E** and S2H).

Variation in autophagy levels between different AMLs independently of the differentiation status

Next we analyzed the expression of autophagy genes and the functional consequences in patients AML $CD34^+$ cells. In total 51 AML patients were studied; the clinical characteristics of this cohort are described in Supplementary Table S2 and S3. For studying a homogenous AML cell population *in vitro*, the $CD34^+$ AML subfraction was sorted and analyzed. Quantitative PCR studies demonstrated that essential autophagy genes ATG5 and ATG7 are more highly expressed in a subset of AMLs compared to $CD34^+$ normal bone marrow cells (S3A and Supplementary Table S4). In addition, expression levels of autophagy genes in AML and normal bone marrow was assessed in publicly available expression datasets (Bloodspot expression database[30]). Expression of a subgroup of autophagy genes was higher in AML compared to normal HSCs, especially genes involved in the mTOR dependent ULK1 complex or LC3 lipidation (S3B).[30] To investigate the functional consequences of this observation, we measured autophagy flux in AML $CD34^+$ cells (n=51). A large variability in autophagic-flux was observed, comparable to the results in cell lines (**Fig 3A** and **Fig 1**, S3C). No difference in autophagic flux was observed between the AML $CD34^+CD38^-$ fraction compared to more mature $CD34^+CD38^+$ fraction (n=8, S3D). Also, no difference was observed between bone marrow and peripheral blood-derived AML cells (S3E)**.** Since AML is clinically a heterogeneous disease, autophagic flux was correlated to a number of clinical relevant parameters including, the French-American-British classification (FAB), cytogenetics, molecular markers, and prognostic risk classification. No significant difference in autophagy flux was shown between AML cells belonging to the myeloid (M1-M2) or monocytic lineages (M4-M5) (S3F)**.** Cytogenetic analysis revealed that AML patients with complex cytogenetic abnormalities had the highest level of autophagy (**Fig 3B**). In line with

these results, expression of many core autophagy genes was higher in AMLs with complex karyotype compared to other AML subgroups (S3B).[30] When patients were categorized according to ELN criteria[31] in favorable, intermediate-I, -II and adverse risk-groups, AML CD34$^+$ cells belonging to adverse-risk group had significantly higher levels of autophagy compared to the intermediate- or favorable-risk AMLs **(Fig 3C).** AMLs with mutations in TP53, which were all classified as adverse-risk, had higher autophagic flux **(Fig 3D).** In contrast, no differences in autophagy levels were observed in AMLs harboring mutations in FLT3, NPM1, IDH1/2, DNMT3A or CEPBA genes **(Fig 3D)**.

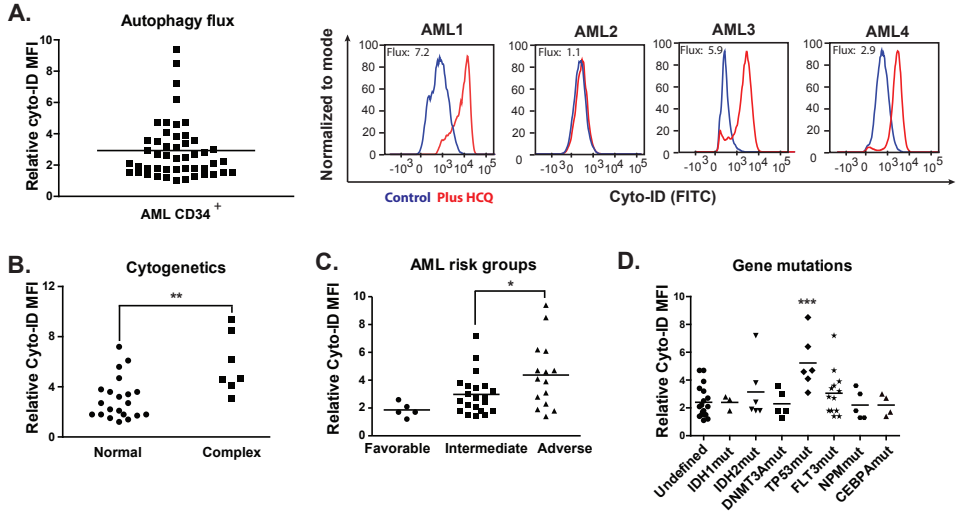

Figure 3. Variation in autophagy levels between different AMLs, independent of the differentiation status. (A) Left panel, for autophagic flux measurements (relative Cyto-ID accumulation) in AML CD34$^+$ blasts (n=51), AML CD34+ cells were cultured for 3 days on MS5 stromal layer before overnight incubation with 20 μM HCQ. Right panel, representative FACS plot showing the accumulation of Cyto-ID after treatment with HCQ. **(B)** Autophagy flux in AMLs with normal karyotype vs. complex cytogenetic abnormalities. **(C)** Autophagy flux in AMLs according to the various ELN risk groups. **(D)** Autophagy flux in AML CD34$^+$ cells according to commonly mutated genes in AML.
Error bars represent SD; *, ** or *** represents p<.05, p<.01 or p<.001, respectively.

To study the functional relevance of the autophagic flux for survival, AML CD34+ cells were treated with 0, 5, 10 or 20 μM HCQ for 72 hrs. The survival of AML cells was measured over time and compared to normal bone marrow CD34+ cells treated in a similar manner. As shown in **Figure 4A,** a significant dose-dependent increase in sensitivity to HCQ was observed in AML CD34+ compared to CD34+ cells isolated from healthy controls (20 μM HCQ, 23.0 ± 3.1% vs 42.5 ± 6.6% surviving cells, respectively, $P<0.05$). Similarly, inhibition of autophagy in AML CD34+ cells resulted in a dose-dependent increase in apoptosis as measured by Annexin-V positivity (**Fig 4B** and S4A**).**

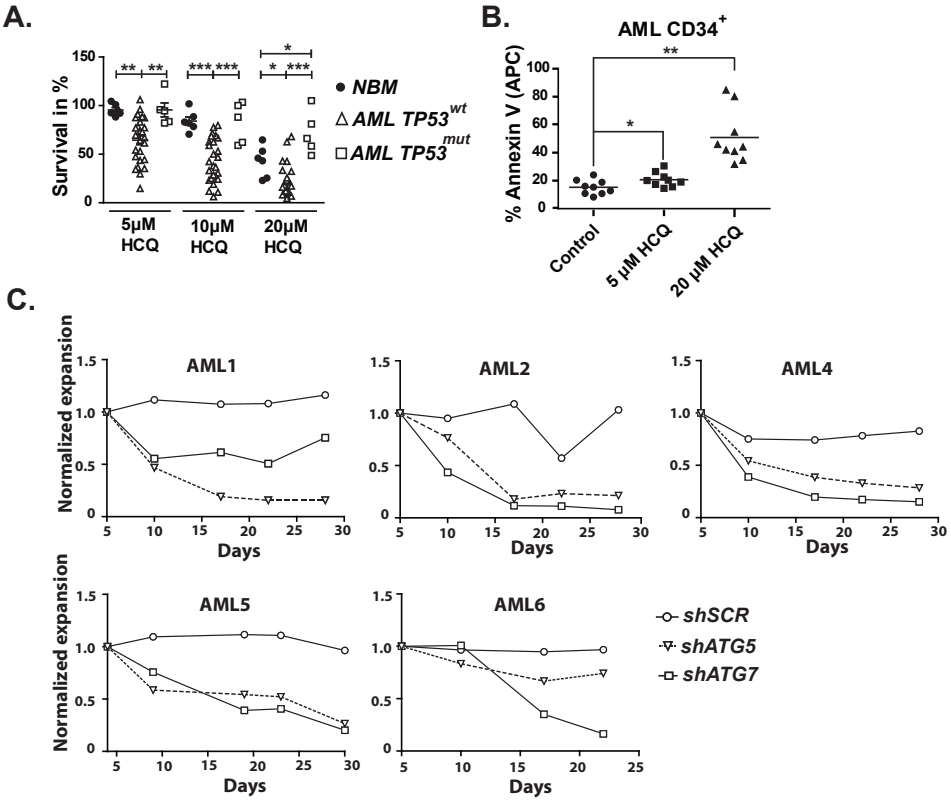

Figure 4. Inhibition of autophagy triggers apoptosis in primary AML CD34+ cells. (**A**) Survival of normal bone marrow (NBM) CD34+, TP53wt AML CD34+ or TP53mut AML CD34+ cells were cultured for 3 days on a MS5 stromal layer before treated with 5, 10 or 20 μM HCQ for 48 hrs. (**B**) Quantification of Annexin V percentages in AML (n=9) after treatment with 5 or 20 μM HCQ. (**C**) Normalized expansion of AML CD34+ cells transduced with shSCR, shATG5 or shATG7, cultured on a MS5 stromal layer.
Error bars represent SD; *, ** or *** represents p<.05, p<.01 or p<.001, respectively.

In contrast to observations in leukemic cell lines, no correlation was observed between the level of autophagic flux and the sensitivity for HCQ. To validate the dependency on autophagy in an alternative manner, AML CD34$^+$ (n=5) were transduced with either shATG5 or shATG7, and expansion on a MS5 stromal layer was measured over time. A strong decrease in cell expansion was observed in response to ATG5 or ATG7 downregulation in comparison to shSCR transduced AML cells (**Fig 4C,** S4B and S4C).

Inhibition of autophagy triggers a p53-dependent increase in apoptosis in AML CD34$^+$ cells

Since we observed that some AML CD34$^+$ samples were less sensitive for HCQ, we compared the sensitivity of wild type TP53 (TP53^{wt}) to those harboring TP53 mutations (TP53^{mut}). As shown in **Fig 4A**, TP53^{mut} AML CD34$^+$ cells (n=5, Supplementary Table S3) were significantly less sensitive at 5, 10 or 20 μM HCQ compared to TP53^{wt} cells (20 μM HCQ, 71.8. ± 9.8% vs. 23.0 ± 3.1% surviving cells respectively, P<0.0001). To characterize further differences in responsiveness between TP53^{wt} and TP53^{mut} patient-derived cells, AML CD34$^+$ TP53^{wt} cells (n=5) or TP53^{mut} cells (n=4) were treated with HCQ, and p53-dependent transcriptional target gene expression patterns were analyzed. In patients with TP53 mutations both homozygous and heterozygous TP53 mutations were observed. Basal levels of BAX, PUMA and p21 mRNA expression were lower in TP53^{mut} cells compared to TP53^{wt} AML CD34$^+$ cells. Interestingly, in contrast to TP53^{wt} cells, expression levels of pro-apoptotic BAX and PUMA were not increased upon HCQ treatment in TP53^{mut} AML CD34$^+$ cells, suggesting that the apoptotic response was severely dampened in these cells (**Fig 5A**). To confirm the role of p53 in the HCQ mediated effects, TP53^{wt} AML cells were co-treated with Nutlin-3A, which stabilizes p53 by inhibition of MDM2. The combined use of HCQ and Nutlin-3A significantly enhanced the apoptotic effect compared to HCQ alone in TP53^{wt} AML CD34$^+$ cells (**Fig 5B**). To verify these findings in an alternative manner p53^{wt} and mutant TP53^{R273H} were overexpressed in p53^{wt} OCIM3 leukemic cells and subsequently treated them with increasing concentrations of HCQ. TP53^{R273H} is described as gain-of-function mutation associated with drug resistance. Overexpression of p53^{wt} enhanced the HCQ-dependent apoptotic response and resulted in reduced survival compared to control (S5A). In contrast, overexpression of mutant TP53^{R273H} rendered the AML cells more resistant to HCQ treatment (**Fig 5C,** S5A). However, overexpression of p53^{wt} or TP53^{R273H} in OCIM3 cells did not affect the autophagic flux as determined by Cyto-ID (S5B)**.** Comparable results were obtained in the context of p53 knockdown in OCIM3 and MOLM13 cells. No change in accumulation of LC3-II or SQSTM1/p62 was observed. **(Fig 5D** and S5C**).** Also in normal CB CD34$^+$ cells overexpression of p53^{wt} or TP53^{R273H}, did not affect the levels of autophagy (Relative Cyto-ID values; control 2.3 ± 0.4 fold, p53^{wt} 2.2 ± 0.6 fold or p53^{mut} 2.1 ±

0.3 fold). Together, these results indicate that inhibition of autophagy initially triggers a p53-dependent apoptotic response, which is severely dampened in AML CD34$^+$ cells harboring mutations in the TP53 gene irrespective of the autophagy flux.

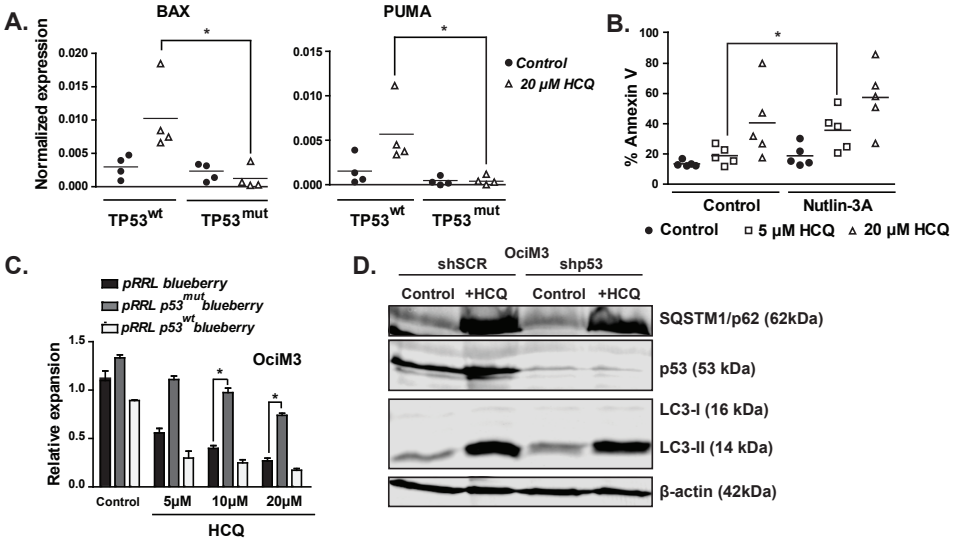

Figure 5. TP53 mutant AMLs are resistant for HCQ induced apoptosis. **(A)** Gene expression of BAX and PUMA determined by quantative RT-PCR in TP53wt (n=4) or TP53mut (n=4) AMLs. AML CD34+ cells were cultured for 3 days on a MS5 stromal layer before 72 hours incubation with 20 μM HCQ. **(B)** Percentage of Annexin V$^+$ positive cells in TP53wt AML CD34+ cells treated with 5 or 20 μM HCQ in conjunction with or without Nutlin-3A. **(C)** Cell counts of OCIM3 cells transduced with pRRL-mBlueberry, pRRL-P53mut-mBlueberry or pRRL-P53wt-mBlueberry, treated with different concentrations of HCQ. **(D)** Western blot showing LC3-II, SQSTM1/p62 and p53 protein expression in OCIM3 cells transduced with shSCR or shP53 treated overnight with or without 20 μM HCQ.
Error bars represent SD; * represents p<.05.

AML CD34$^+$ROS^{low} cells have a higher autophagic flux

We did not observe differences in autophagy in more immature CD34$^+$CD38$^-$ vs more mature CD34$^+$CD38$^+$ blast (S3D). To determine whether there is still variability in the level of autophagy within the AML CD34$^+$ fraction, we separated the AML CD34$^+$ subfraction into ROS^{low} and ROS^{high} cells. A recent study has shown that ROS^{low} AML cells are enriched for leukemic stem cells (LSC) by using *in vitro* as well as *in vivo* assays.[32] We identified the ROS^{low} and ROS^{high} AML CD34$^+$ by sorting the 15% low and high subfractions based on the CellROX mean fluorescent intensity (MFI) in the AML CD34$^+$ cell population **(Fig 6A)**. A significant distinction in CellROX MFI was demonstrated in AML CD34$^+$ (n=14) ROS^{high} compared

to ROS^{low} cells (**Fig 6A,** S6A)**.** Sorted ROS^{low} cells exhibited more immature morphology, as determined by the relative size of the nucleus to the cytoplasm. Representative pictures of AML cells from sorted ROS^{low} and ROS^{high} AMLs are shown in S6B. Interestingly, ROS^{low} cells maintained a significantly higher autophagic flux compared to the ROS^{high} AML $CD34^+$ cells, within the same patient sample, as determined by Cyto-ID (**Fig 6B**, $P<0.01$, S6C). In addition, sorted ROS^{low} and ROS^{high} subfractions AML $CD34^+$ cells were treated overnight with HCQ and subsequently accumulation LC3-II was detected by Western blotting. A higher accumulation was shown in the ROS^{low} AML cells (S6D). qRT-PCR analysis demonstrated a significantly higher expression of BCL-2 in the ROS^{low} AML $CD34^+$ cells (S6E). In addition, higher expression of the autophagy genes Beclin-1 and LC3 and the autophagy regulator FOXO3A was observed in ROS^{low} AML $CD34^+$ cells compared to the ROS^{high} $CD34^+$ cells (**Fig 6C).**[33, 34] In contrast, expression of other key autophagy genes and major ROS scavengers such as SOD1, SOD2 and Catalase was comparable between both fractions (data not shown).

To evaluate growth characteristics and the functional relevance of autophagy in the distinct AML $CD34^+$ subpopulations (n=4), FACS-sorted AML $CD34^+$ ROS^{low} and ROS^{high} cells were cultured on MS5 bone marrow stromal cells. The ROS^{low} AML $CD34^+$ cells exhibited long-term expansion in comparison with the ROS^{high} $CD34^+$ cells (week 5; ROS^{low} 7.1 fold ± 2.1 vs ROS^{high} 1.6 fold ± 0.4 (n=6, P=<0.05)). Next, ROS^{low} and ROS^{high} fractions were treated with 5 or 20 μM HCQ for 48 hours and survival was determined (**Fig 6D**). ROS^{low} cells were more sensitive to HCQ treatment compared to ROS^{high} cells, correlating with increased apoptosis (S6F)**.** Since mitochondria have an important role in ROS production, we evaluated mitochondrial mass in AML $CD34^+$ cells in both the ROS^{low} and ROS^{high} subfractions. AML $CD34^+$ ROS^{low} cells had a lower mitochondrial mass compared to ROS^{high} AML $CD34^+$ cells (n=11, p<0.0001, S6G).

Knockdown of ATG5 inhibits myeloid leukemia maintenance in vivo

Based on the observations that ATG5 and ATG7 knockdown reduce the expansion of AML $CD34^+$ cells *in vitro*, we determined whether this would also occur *in vivo.* To exclude the possibility that the knockdown of ATG5 or ATG7 affected cell migration, *in vitro* transwell experiments were performed with the OCIM3 and MLOM13 cell line. In both cell lines, the SDF1 mediated migration was not affected by the knockdown of ATG5 or ATG7 (S7D). Subsequently AML $CD34^+$ cells were transduced with the shATG5 or shSCR-GFP and transplanted in immunodeficient NSG mice, as outlined in **Fig 7A.** Transplanted AML blasts were at least 14% GFP positive at time of injection (S7A) and ATG5 knockdown was confirmed by qRT-PCR (S7B-C).

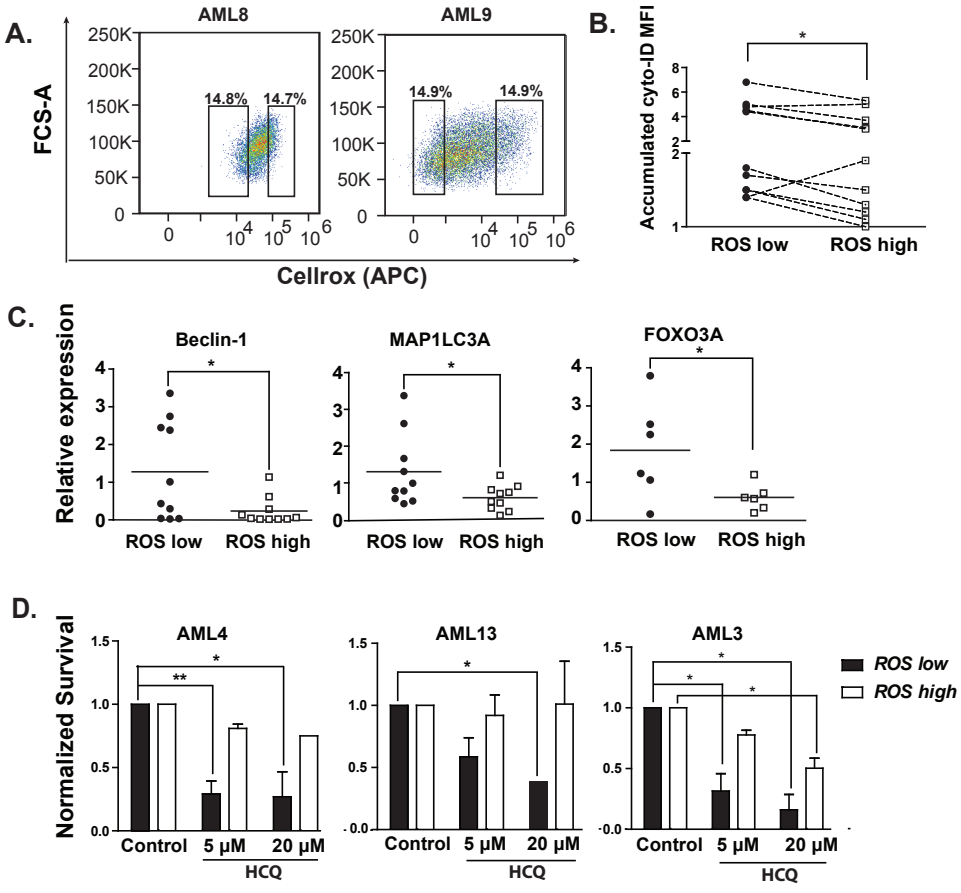

Figure 6 Autophagy is higher in the ROSlow population of AML blasts. **(A)** Representative FACS plots showing CellROX staining in freshly isolated AML CD34+ cells. **(B)** Relative Cyto-ID levels in ROShigh and ROSlow fractions of AML CD34+ cells (n=11). **(C)** Gene expression of Beclin-1 and LC3 in freshly sorted AML CD34+ROShigh and CD34+ROSlow cells. **(D)** Survival of FACS sorted ROShigh and ROSlow AML CD34+ cells, cultured for 3 days on a MS5 stromal layer before treated for 48 hours with different concentrations HCQ.
Error bars represent SD; *, ** or *** represents p<.05, p<.01 or p<.001, respectively.

The time for the onset of leukemia was determined by measuring the percentage of huCD45 in peripheral blood. While GFP levels for shSCR remained stable at around ~15%, the contribution of the shATG5 transduced cells to the engrafted AML cells was significantly reduced, starting from week 6 (**Fig 7B,** S7E). After sacrifice, we observed high engraftment levels in bone marrow, spleen and liver as determined by the percentage of CD45. The contribution of shSCR-GFP transduced cells within the CD45 compartment was stable

around ~20% in all studied organs. On the contrary, the percentage of shATG5-GFP transduced cells within the CD45 compartment was strongly decreased (**Fig 7C**). The engrafted human AML cells were all of myeloid origin, as determined by CD33 expression (S7F). These results demonstrate that autophagy is also essential for leukemia maintenance *in vivo*.

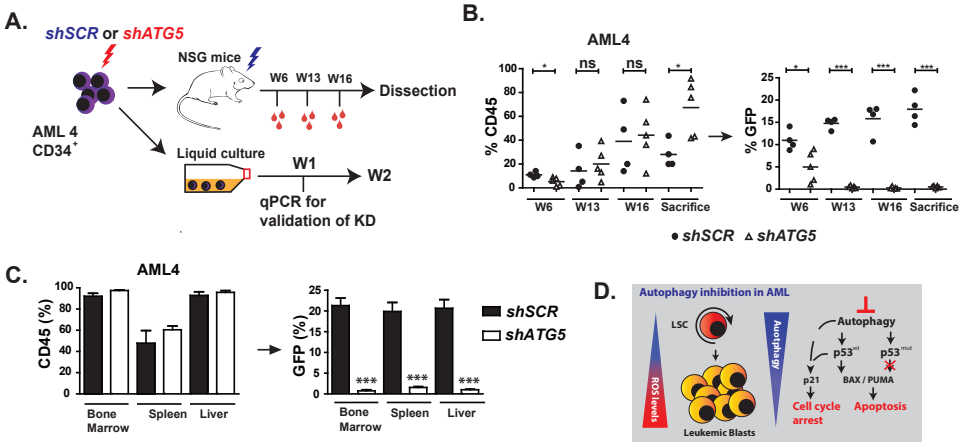

Figure 7. Knockdown of ATG5 in AML CD34+ blasts results in impaired engraftment. (A) Experimental set-up. **(B)** Left panel: engraftment levels measured by huCD45%. Right panel: the GFP% within huCD45+ population. Each dot represents data from a single mouse, shSCR (N=4) and shATG5 (N=5). **(C)** Engraftment (percentage huCD45) at time of sacrifice in bone marrow, spleen and liver and the GFP% within the huCD45+ population. **(D)** Summarizing Model: LSCs are enriched in the ROSlow fraction of AML blasts. ROSlow cells maintain a higher basal autophagy flux and have a lower mitochondrial mass compared to ROShigh cells. Right part: short-term genetic or pharmaceutical Inhibition of autophagy triggered a p53 dependent apoptotic response in p53 wild type AMLs, which was severely dampened in p53 mutant AMLs.
Error bars represent SD; * or *** represents p<.05 or p<.001, respectively.

DISCUSSION

The aim of our study was to determine whether inhibiting autophagy can provide an alternative means to impair LSC functionality. AML CD34^{+} cells were susceptible for autophagy inhibition, which was demonstrated by *in vitro* and *in vivo* experiments. *In vitro* studies indicated that the subfraction of ROS^{low} AML CD34^{+} cells had the highest autophagic flux and were more susceptible to HCQ treatment when compared to ROS^{high} AML CD34^{+} cells. The AML ROS^{low} subfraction is further characterized by lower mitochondrial mass

and elevated BCL-2, FOXO3A and Beclin-1 expression. These results are of interest since a previous study has shown that ROS^{low} AML CD34^{+} cells are enriched for LSCs.[32] Similar, murine ROS^{low} HSPC are enriched for stem cells.[35] In the studied AMLs, the autophagy-flux was most-pronounced in adverse-risk group with complex cytogenetic abnormalities which are frequently associated with TP53 mutations. Transcriptome data revealed a significant higher expression of autophagy genes in the AML subgroup with complex karyotype. It has been suggested that the adverse-risk AMLs have a higher number of LSCs compared to favorable-risk AMLs, which might have consequences for the measured level of autophagy.[36, 37] Although the high autophagy flux was connected with complex karyotype and TP53 mutations, modulation of p53 in normal or leukemic cells by p53 knockdown or ectopic overexpressing p53^{mut} did not affect the autophagy flux. Therefore, the high autophagic flux in the AML CD34^{+} subfraction might be an intrinsic property as consequences of an adaptive response to constitutive metabolic stress linked to the (epi)genetic mutations.

Inhibition of autophagy in leukemic cells might limit nutrient availability in cells, causing metabolic stress and consequently apoptosis. Moreover, impaired autophagy in hematopoietic cells has been associated with increased mitochondrial mass, resulting in ROS accumulation.[8,9,15] In turn, excessive ROS has been shown to cause oxidative DNA damage and consequently premature senescence and HSC exhaustion.[38,39] Our study indicates that the p53 pathway, irrespective of the level of autophagy, is an important effector pathway for cell death induced by autophagy inhibition, which has consequences for AMLs with TP53 mutations. TP53^{mut} AML cells show decreased sensitivity for short-term treatment with HCQ and an impaired upregulation of the apoptotic genes PUMA and BAX, indicating that the initial apoptotic response in these cells is strongly impaired.

In view of these findings co-treatment with autophagy inhibitors might only be a promising approach for the treatment of TP53^{wt} AMLs. Similar observations have been made in chronic myeloid leukemia (CML).[40, 41] The combination of tyrosine kinase inhibitors in combination with autophagy inhibitors resulted in more effective elimination of CML stem cells.[42] This approach might also be attainable *in vivo* since various studies in patients with solid tumors have shown that high dose HCQ can block autophagy *in vivo*.[17, 23, 43, 44] Currently, a second generation of HCQ-derived autophagy inhibitors are being developed, which are more potent in inhibition of autophagy[45, 46], thereby increasing the clinical applicability of autophagy inhibition.

In the present study we focused mainly on the role of autophagy during leukemia maintenance. This might be distinct from the role of autophagy during leukemia initiation, as consequences of the emergence of (epi)genetic mutations.[2, 3] Model systems for leukemia and solid tumors have shown that during malignant transformation, autophagy might be reduced as result of

mutagenesis, resulting in accumulation of mitochondria, ROS-mediated DNA damage and activation of NF-κB signalling.[12,13] Likewise, U2AF35 mutations in myelodysplastic syndrome cause abnormal processing of ATG7 pre-mRNA and consequently reduced expression of ATG7.[47] In addition a recent study reported mutations of autophagy genes in a small fraction of MDS patients, which might be contributive to malignant transformation.[48]

In summary, our results demonstrate that autophagy has a critical function for AML maintenance and that inhibition of autophagy might be a promising therapeutic strategy in a subgroup of AML patients (summarizing model**, Fig 7D**).

REFERENCES

1. Shen Y, Zhu Y-M, Fan X, Shi JY, Wang QR, Yan XJ *et al.* Gene mutation patterns and their prognostic impact in a cohort of 1185 patients with acute myeloid leukemia. *Blood* 2011; **118:** 5593-5603.

2. Wouters BJ, Delwel R. Epigenetics and approaches to targeted epigenetic therapy in acute myeloid leukemia. *Blood* 2016; **127:** 42-52.

3. Rose D, Haferlach T, Schnittger S, Takahashi N, Yamashita T. Subtype-specific patterns of molecular mutations in acute myeloid leukemia. *Leukemia* 2017; **31**: 11-17.

4. Testa U, Riccioni R. Deregulation of apoptosis in acute myeloid leukemia. *Haematologica* 2007; **92:** 81-94.

5. Bosman MCJ, Schepers H, Jaques J, Brouwers-Vos AZ, Quax WJ, Schuringa JJ *et al.* The TAK1-NF-κB axis as therapeutic target for AML. *Blood* 2014; **124:** 3130-3140.

6. Yang Z, Klionsky DJ. Eaten alive: a history of macroautophagy. *Nat Cell Biol* 2010; **12:** 814-822.

7. Ashrafi G, Schwarz TL. The pathways of mitophagy for quality control and clearance of mitochondria. *Cell Death Differ* 2013; **20:** 31-42.

8. Joshi A, Kundu M. Mitophagy in hematopoietic stem cells: The case for exploration. *Autophagy* 2013; **9:** 1737-1749.

9 Gomez-Puerto MC, Folkerts H, Wierenga AT, Schepers K, Schuringa JJ, Coffer PJ *et al.* Autophagy proteins ATG5 and ATG7 are essential for the maintenance of human CD34(+) hematopoietic stem-progenitor cells. *Stem Cells* 2016**;** **34**: 1651-1663.

10. Salemi S, Yousefi S, Constantinescu, MA, Fey MF, Simon HU. Autophagy is required for self-renewal and differentiation of adult human stem cells. *Cell Res* 2012; **22:** 432-435.

11. Mortensen M, Soilleux EJ, Djordjevic G, Tripp R, Lutteropp M, Sadighi-Akha E *et al.* The autophagy protein Atg7 is essential for hematopoietic stem cell maintenance. *J Exp Med* 2011; **208:** 455-467.

12. Watson AS, Riffelmacher T, Stranks A, Williams O, De Boer J, Cain K *et al.* Autophagy limits proliferation and glycolytic metabolism in acute myeloid leukemia. *Cell Death Discov* 2015; **1:** 15008.

13. Cao Y, Zhang S, Yuan N, Wang J, Li X, Xu F *et al.* Hierarchal Autophagic Divergence of Hematopoietic System. *J Biol Chem* 2015; **290:** 23050-23063.

14. Mortensen M, Ferguson DJP, Edelmann M, Kessler B, Morten KJ, Komatsu M *et al.* Loss of autophagy in erythroid cells leads to defective removal of mitochondria and severe anemia in vivo. Proc. Natl Acad. Sci. U S A 2010; **107:** 832-837.

15. Luo C, Li Y, Wang H, Feng Z, Li Y, Long J, Liu J et al. Mitochondrial accumulation under oxidative stress is due to defects in autophagy. J Cell Biochem 2013; **114**: 212-9.

16. Stankov MV, El Khatib M, Kumar Thakur B, Heitmann K, Panayotova-Dimitrova D, Schoening J *et al.* Histone deacetylase inhibitors induce apoptosis in myeloid leukemia by suppressing autophagy. *Leukemia* 2014; **28:** 577-588.

17. Sehgal AR, Konig H, Johnson DE, Tang D, Amaravadi RK, Boyiadzis M *et al.* You eat what you are: autophagy inhibition as a therapeutic strategy in leukemia. *Leukemia.* 2015; **29:** 517-525.

18. Piya S, Kornblau SM, Ruvolo VR, Mu H, Ruvolo PP, McQueen T *et al.* Atg7 suppression enhances chemotherapeutic agent sensitivity and overcomes stroma-mediated chemoresistance in acute myeloid leukemia. *Blood* 2016; **128**: 1260-1269.

19. Altman JK, Szilard A, Goussetis DJ, Sassano A, Colamonici M, Gounaris E *et al.* Autophagy Is a Survival Mechanism of Acute Myelogenous Leukemia Precursors during Dual mTORC2/mTORC1 Targeting. *Clin Cancer Res* 2014; **20:** 2400-2409.

20. Liu L-L, Long Z-J, Wang L-X, Zheng FM, Fang ZG, Yan M *et al.* Inhibition of mTOR Pathway Sensitizes Acute Myeloid Leukemia Cells to Aurora Inhibitors by Suppression of Glycolytic Metabolism. *Mol Cancer Res* 2013; **11:** 1326-1336.

21. Martelli AA, Evangelisti C, Chiarini F, McCubrey JA. The Phosphatidylinositol 3-kinase/AKT/mTOR signaling network as a therapeutic target in acute myelogenous leukemia patients. *Oncotarget.* 2010; **1**: 89-103.

22. Torgersen ML, Engedal N, Bøe S-O, Hokland P, Simonsen A. Targeting autophagy potentiates the apoptotic effect of histone deacetylase inhibitors in t(8;21) AML cells. *Blood* 2013; **122:** 2467-2476.

23. Mahalingam D, Mita M, Sarantopoulos J, Wood L, Amaravadi RK, Davis LE *et al.* Combined autophagy and HDAC inhibition: A phase I safety, tolerability, pharmacokinetic, and pharmacodynamic analysis of hydroxychloroquine in combination with the HDAC inhibitor vorinostat in patients with advanced solid tumors. *Autophagy* 2014; **10**: 1403-1414.

24. Liu L, Yang M, Kang R, Wang Z, Zhao Y, Yu Y *et al.* HMGB1-induced autophagy promotes chemotherapy resistance in leukemia cells. *Leukemia* 2011; **25:** 23-31.

25 Sumitomo Y, Koya J, Nakazaki K, Kataoka K, Tsuruta-Kishino T, Morita K *et al.* Cytoprotective autophagy maintains leukemia-initiating cells in murine myeloid leukemia. Blood 2016; **128**: 1614-1624

26 Van Gosliga D, Schepers H, Rizo A, van der Kolk D, Vellenga E, Schuringa JJ. Establishing long-term cultures with self-renewing acute myeloid leukemia stem/progenitor cells. *Exp Hematol.* 2007 **35**: 1538-1549.

27. Ai H-w, Shaner NC, Cheng Z, Tsien RY, Campbell RE. Exploration of New Chromophore Structures Leads to the Identification of Improved Blue Fluorescent Proteins. *Biochemistry* 2007; **46:** 5904-5910.

28. Korthuis PM, Berger G, Bakker B, Rozenveld-Geugien M, Jaques J, de Haan G *et al.* CITED2-mediated human hematopoietic stem cell maintenance is critical for acute myeloid leukemia. *Leukemia* 2015; **29:** 625-635.

29. Klionsky DJ, Abdelmohsen K, Abe A, Abedin MJ, Abeliovich H, Acevedo Arozena A *et al.* Guidelines for the use and interpretation of assays for monitoring autophagy (3rd edition). *Autophagy* 2016; **12:** 1-222.

30. Bagger FO, Sasivarevic D, Sohi SH, Laursen LG, Pundhir S, Sønderby CK *et al.* BloodSpot: a database of gene expression profiles and transcriptional programs for healthy and malignant haematopoiesis. *Nucleic Acids Res* 2016; **44**: D917-D924.

31. Döhner H, Estey EH, Amadori S, Appelbaum FR, Büchner T, Burnett AK *et al.* Diagnosis and management of acute myeloid leukemia in adults: recommendations from an international expert panel, on behalf of the European LeukemiaNet. *Blood* 2010; **115:** 453-474.

32. Lagadinou Eleni D, Sach A, Callahan K, Rossi RM, Neering SJ, Minhajuddin M *et al.* BCL-2 Inhibition Targets Oxidative Phosphorylation and Selectively Eradicates Quiescent Human Leukemia Stem Cells. *Cell Stem Cell* 2013; **12:** 329-341.

33. Warr MR, Binnewies M, Flach J, Vervoort SJ, van Boxtel R, Putker M *et al.* FOXO3A directs a protective autophagy program in haematopoietic stem cells. *Nature* 2013; **494:** 323-327.

34. Van der Vos KE, Eliasson P, Proikas-Cezanne T, Vervoort SJ, van Boxtel R, Putker M *et al.* Modulation of glutamine metabolism by the PI(3)K–PKB–FOXO network regulates autophagy. *Nat Cell Biol* 2012; **14:** 829-837.

35. Jang Y-Y, Sharkis SJ. A low level of reactive oxygen species selects for primitive hematopoietic stem cells that may reside in the low-oxygenic niche. *Blood* 2007; **110:** 3056-3063.

36. Griessinger E, Anjos-Afonso F, Vargaftig J, Taussig DC, Lassailly F, Prebet T *et al.* Frequency and Dynamics of Leukemia-Initiating Cells during Short-term Ex Vivo Culture Informs Outcomes in Acute Myeloid Leukemia Patients. *Cancer Res* 2016; **76**: 2082-2086.

37 Pabst C, Bergeron A, Lavallée VP, Yeh J, Gendron P, Norddahl GL *et al.* GPR56 identifies primary human acute myeloid leukemia cells with high repopulating potential in vivo. Blood 2016; **127**: 2018-2027

38. Yahata T, Takanashi T, Muguruma Y, Ibrahim AA, Matsuzawa H, Uno T, Sheng Y *et al.* Accumulation of oxidative DNA damage restricts the self-renewal capacity of human hematopoietic stem cells. *Blood* 2011; **118:** 2941-2950.

39 Nakata S, Matsumura I, Tanaka H, Ezoe S, Satoh Y, Ishikawa J *et al.* NF-kappaB family proteins participate in multiple steps of hematopoiesis through elimination of reactive oxygen species. *J Biol Chem* 2004; **279**: 55578-55586

40. Crowley LC, Elzinga BM, O'Sullivan GC, McKenna SL. Autophagy induction by Bcr-Abl-expressing cells facilitates their recovery from a targeted or nontargeted treatment. *Am J Hematol* 2011; **86:** 38-47.

41. Yu Y, Yang L, Zhao M, Zhu S, Kang R, Vernon P *et al.* Targeting microRNA-30a-mediated autophagy enhances imatinib activity against human chronic myeloid leukemia cells. *Leukemia* 2012; **26:** 1752-1760.

42. Bellodi C, Lidonnici MR, Hamilton A, Helgason GV, Soliera AR, Ronchetti M *et al.* Targeting autophagy potentiates tyrosine kinase inhibitor–induced cell death in Philadelphia chromosome–positive cells, including primary CML stem cells. *J Clin Invest* 2009; **119:** 1109-1123.

43. Rangwala R, Leone R, Chang YC, Fecher LA1 Schuchter LM, Kramer A *et al.* Phase I trial of hydroxychloroquine with dose-intense temozolomide in patients with advanced solid tumors and melanoma. *Autophagy* 2014; **10**: 1369-1379.

44. Vogl DT, Stadtmauer EA, Tan K-S, Heitjan DF, Davis LE, Pontiggia L *et al.* Combined autophagy and proteasome inhibition: a phase 1 trial of hydroxychloroquine and bortezomib in patients with relapsed/refractory myeloma. *Autophagy.* 2014; **10:** 1380-1390.

45. Solomon VR, Hu C, Lee H. Design and synthesis of chloroquine analogs with anti-breast cancer property. *Eur J Med Chem* 2010; **45:** 3916-3923.

46. McAfee Q, Zhang Z, Samanta A, Levi SM, Ma XH, Piao S *et al.* Autophagy inhibitor Lys05 has single-agent antitumor activity and reproduces the phenotype of a genetic autophagy deficiency. Proc Natl Acad Sci U S A 2012; **109:** 8253-8258.

47. Park Sung M, Ou J, Chamberlain L, Simone TM, Yang H, Virbasius

CM *et al.* U2AF35(S34F) Promotes Transformation by Directing Aberrant ATG7 Pre-mRNA 3′ End Formation. *Mol Cell* 2016; **62:** 479-490.

48. Visconte V, Przychodzen B, Han Y, Nawrocki ST, Thota S, Kelly KR. Complete mutational spectrum of the autophagy interactome: a novel class of tuor suppressor genes in myeloid neoplasms. *Leukemia* 2017; **2**: 505-510

SUPPLEMENTARY MATERIAL AND METHODS

Antibodies and reagents

The following anti-human antibodies were used: mouse anti-SQSTM1/p62 (sc-28359) and rabbit (sc-130656) or mouse (sc-47778) anti-Actin, mouse anti-p53 (sc-126) from Santa Cruz (Santa Cruz, CA, USA), Mouse anti-LC3 (5F10, 0231-100) from Nanotools (Munich, Germany) and Mouse anti-Histone H3 was obtained from Abcam (Cambridge, UK), Hydroxychloroquine (HCQ), Bafilomycin-A1 (BafA1), Nutlin-3A, 3-Methyladenine (3-MA) and SBI-0206965 (SB) were obtained from Sigma-Aldrich.

Western blotting

Western blot analysis was performed using standard techniques. In brief, cells were lysed in Laemmli buffer and boiled for 5 min. Equal amounts of total lysate were analyzed by SDS-polyacrilamide gel electrophoresis. Proteins were transferred to polyvinylidene difluoride (PVDF) membrane (Millipore, Billerica, Massachusetts, USA) by semidry electroblotting. Membranes were blocked in Odyssey blocking buffer (Westburg, Leusden, the Netherlands) prior to incubation with the appropriate antibodies according to the manufacturer's conditions. Membranes were washed, incubated with secondary antibodies labeled with alexa680 or IRDye800 (Invitrogen, Breda, the Netherlands) and developed by Oddysee infrared scanner (Li-Cor Biosciences, Lincoln, USA).

Fluorescence and light microscopy

pRRL-LC3-GFP or pRRL-GFP transduced MOLM13 or OCIM3 cell lines were treated for 16 hrs with or without Bafilomycin. Cytospins of cells were stained with DAPI (Nuclear stain), washed with PBS and subsequently analyzed by fluorescent microscopy (Leica DM6000B, Amsterdam, The Netherlands) GFP-puncta, as a measure for autophagy, were quantified using Image J software. Cytospins of sorted ROS low and high cells AML cells were stained with May-Grünwald-Giemsa (MGG) staining and analyzed by microscope (Leica DM3000).

In vivo transplantations into NSG.

Before *in vivo* transplantation, mice were sublethally irradiated (1.0 Gy). Following irradiation, mice received filter sterilized neomycin (3.5g/L) via drinking water for 2 weeks. The mice were injected IV (Lateral tail vein) with 0.5 or 1.0 x 10^6 unsorted $CD34^+$ cells for AML4 and AML5 respectively, which were transduced with shSCR-GFP, or shATG5-GFP. Four to five mice were injected for each group. The transduction levels were >14% or >32% GFP for

AML4 and AML5 respectively, at the time of injection. Human cell engraftment was analyzed in peripheral blood (PB) by FACS analysis with intervals of at least 2 weeks, starting from week 6. PB was collected via submandibular puncture.

Migration assay

Migration assay of shSCR, shATG5 or shATG7 transduced OCIM3 and MOLM13 cells was performed in a transwell system (Corning Costar, Cambridge, UK) with an 8 μm pore size. Three days after transduction, cells were resuspended in 100 μL medium and added to the upper chamber; 600 uL of medium with and without 100 ng/mL stromal derived factor-1 was added to the lower chamber. Cells were incubated for 4 hours at 37°C and migrated and non-migrated cells were counted using counting beads.

SUPPLEMENTARY FIGURES

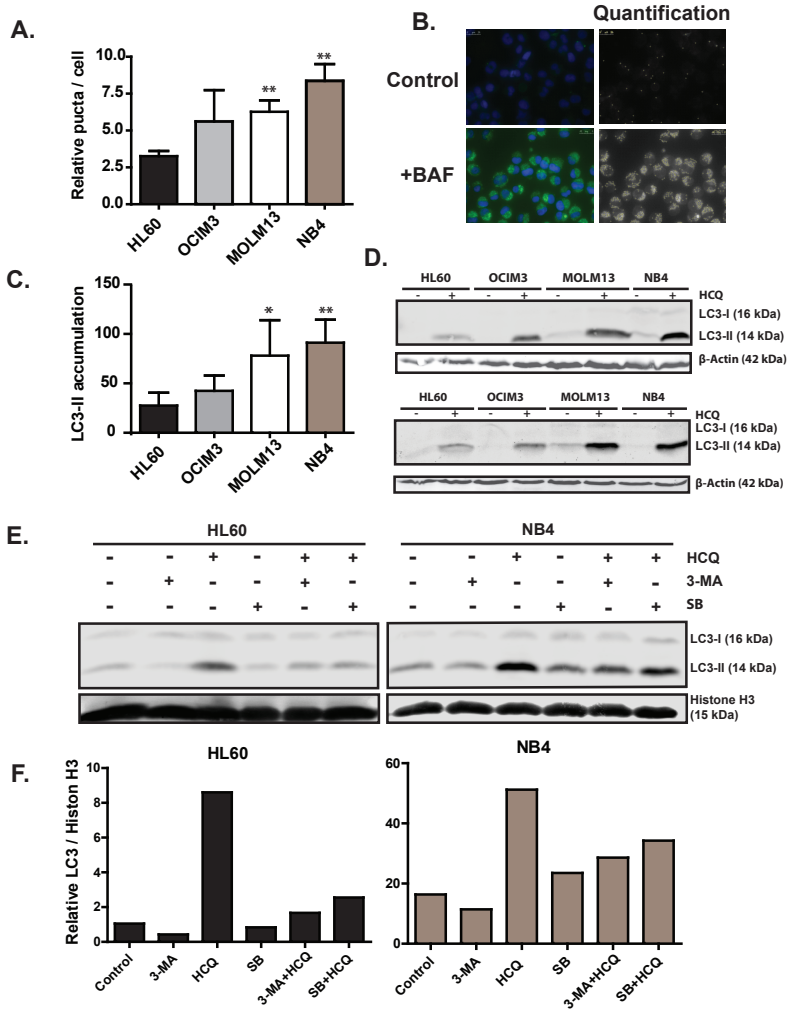

Supplementary figure 1. Variation in autophagy flux between different leukemic cell lines. (A) Leukemic cell lines, expressing LC3-GFP, were treated overnight with or without BAF. LC3-pucta were analysed by fluorescent microscopy. **(B)** Left panels: representative pictures of LC3-GFP expressing cells treated with or without BAF and right panels: quantification of LC3-pucta by ImageJ software. **(C)** Quantification of LC3-II in HL60, OCIM3, MOLM13 and NB4 cells after HCQ treatment (n=4), β-actin was used as loading control. **(D)** Western blots of LC3-II accumulation after overnight 20 μM HCQ treatment in leukemic cell lines, β-actin was used as loading control. **(E)** Western blot showing LC3-II accumulation in HL60 and NB4 cells. HL60 and NB4 cells were pre-treated for 4 hours with PI3K inhibitor (3-MA; 3-Methyladenine) or ULK1 inhibitor (SB; SBI-0206965) before addition of HCQ. Histone H3 was used as control. **(F)** Quantification of LC3-II levels corrected for Histone H3 levels. Error bars represent SD; *, or ** represents p<.05 or p<.01 respectively.

A.

	Knockdown efficiency for shATG5, shATG7 and shP53			
	shSCR	shATG5 (ATG5)	shATG7 (ATG7)	shP53 (p53)
HL60	1,0	0,22 **	0,54 *	na
MOLM13	1,0	0,42 *	0,44 *	0,03 **
OCIM3	1,0	0,25 **	0,63	na
NB4	1,0	0,11 ***	0,41*	0,15 *

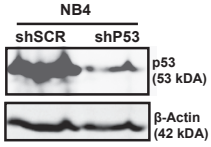

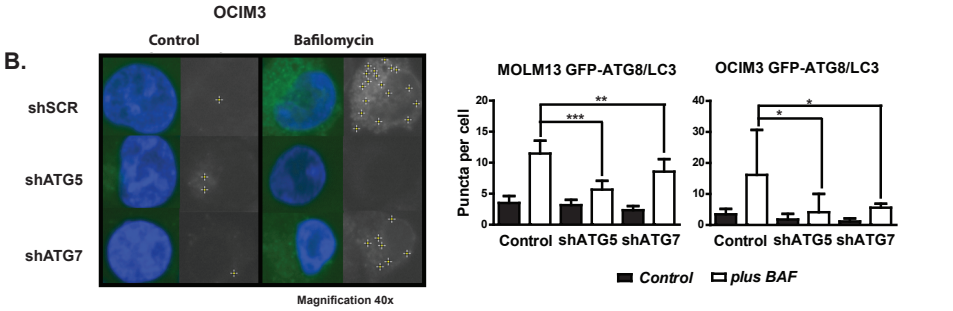

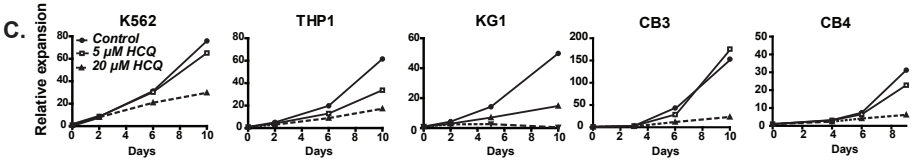

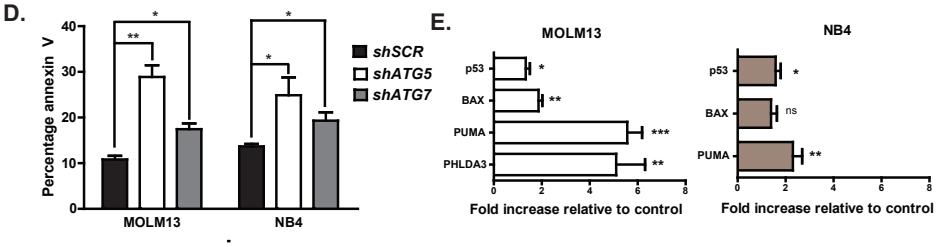

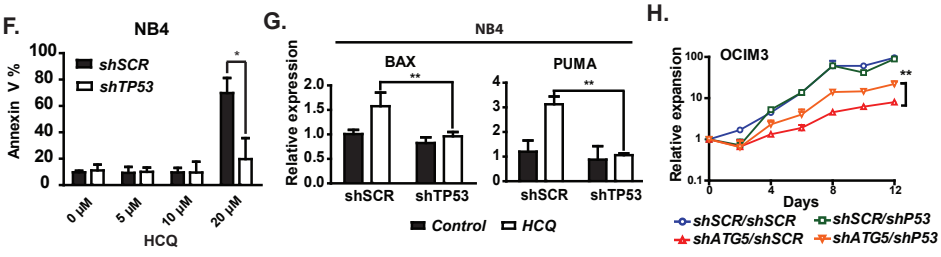

Supplementary figure 2. Correlation between autophagy flux and sensitivity for inhibition of autophagy in leukemic cells. **(A)** Left panel: table showing relative expression of ATG5, ATG7 or p53 as determined by q-PCR in shSCR, shATG5, shATG7 and shP53 transduced cell lines or right panel: p53 protein level after lentiviral transduction with shSCR or shP53 in NB4 cells. **(B)** Left panel: Representative pictures of LC3 puncta in OCIM3 cells transduced with shSCR, shATG5 or shATG7 at day 5 after transduction, treated overnight with or without Bafilomycin-1A (40x magnification). Right panels: Quantification of LC3 puncta in Molm13 and OCIM3, transduced with shSCR, shATG5 or shATG7. **(C)** Relative expansion of leukemia cell lines cells and CB CD34+ cells cultured for 10 days in the presence of different concentrations of HCQ. **(D)** Annexin V levels in Molm13 and NB4 cells at day 5 after knockdown of ATG5 or ATG7, compared to scrambled control. **(E)** Fold increased expression measured by q-RT-PCR, of P53, BAX, PUMA and PHLDA3 after 4 days 20 μM HCQ treatment in MOLM13 and NB4 compared to untreated control. **(F)** Percentage of Annexin V positive cells in shSCR or shp53 transduced NB4 cells, at day 4 after treatment with different concentrations of HCQ. **(G)** q-RT-PCR for BAX and PUMA in shSCR and shP53 transduced NB4 cells, treated with 20 μM HCQ for 4 days. **(H)** Cell expansion in time of OCIM3 cells double transduced with shp53-GFP or shSCR-GFP in combination with shSCR-mCherry or shATG5-mCherry.
Error bars represent SD; *, ** or *** represents $p<.05$, $p<0.01$ or $p<.001$ respectively.

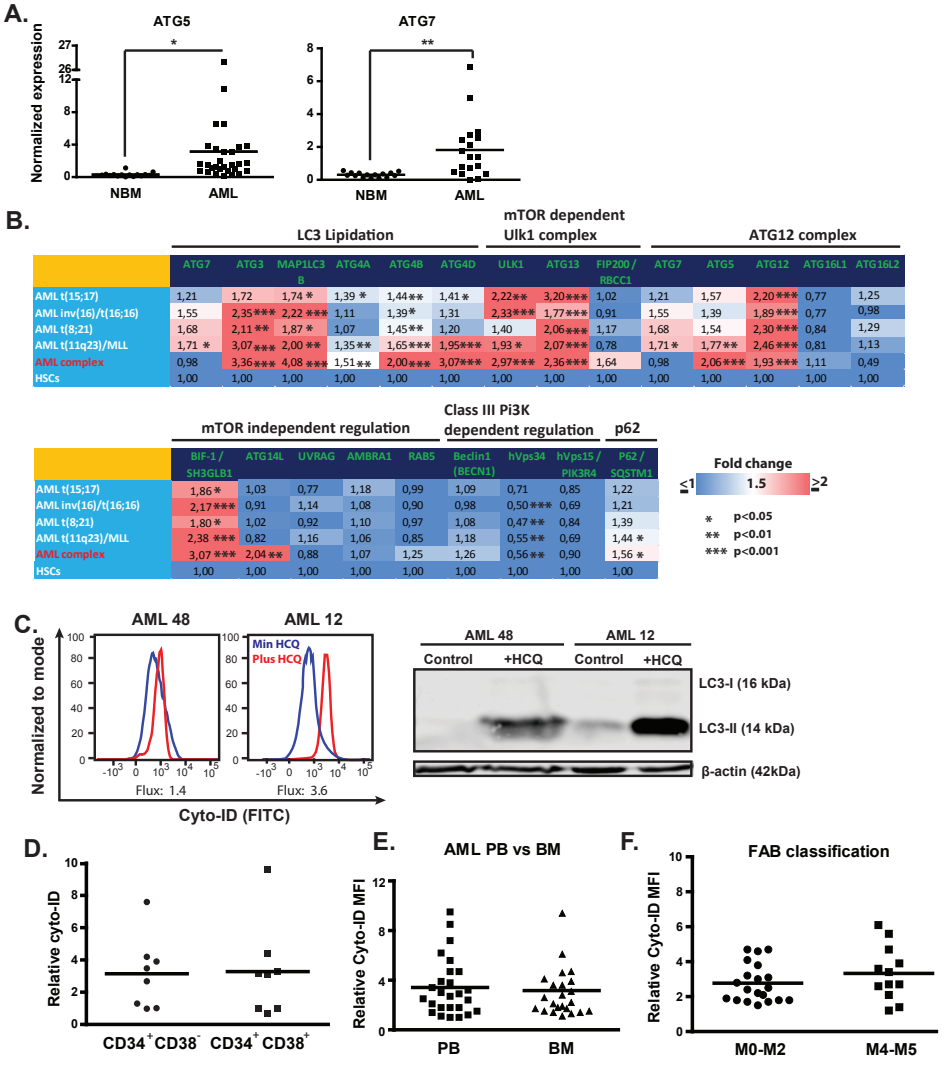

Supplementary figure 3. Variation in autophagy levels between different AMLs, independent of the differentiation status. **(A)** Normalized gene expression of ATG5 and ATG7 in AML CD34+ cells compared to NBM CD34+ cells. **(B)** Heat-map showing fold-change gene expression of autophagy genes in different subtypes of AMLs, relative to expression in normal HSCs. All displayed expression data was acquired from the publicly available expression database; Bloodspot.30. **(C)** Left panels: relative Cyto-ID values or right panels: LC3-II accumulation on Western blot of two AML CD34+ samples treated overnight with or without 20 μM HCQ. **(D)** Relative Cyto-ID measurements in sorted CD34+CD38- and CD34+CD38+ AML blasts after 3 days of culturing on MS5 stroma. **(E)** Relative Cyto-ID measurements in AML CD34+ cells derived from bone marrow (BM) or peripheral blood (PB). **(F)** Autophagy flux in AML cells with myeloid (M0-M2) or monocytic background (M4-5).
Error bars represent SD; *, ** or *** represents p<.05, p<0.01 or p<.001 respectively.

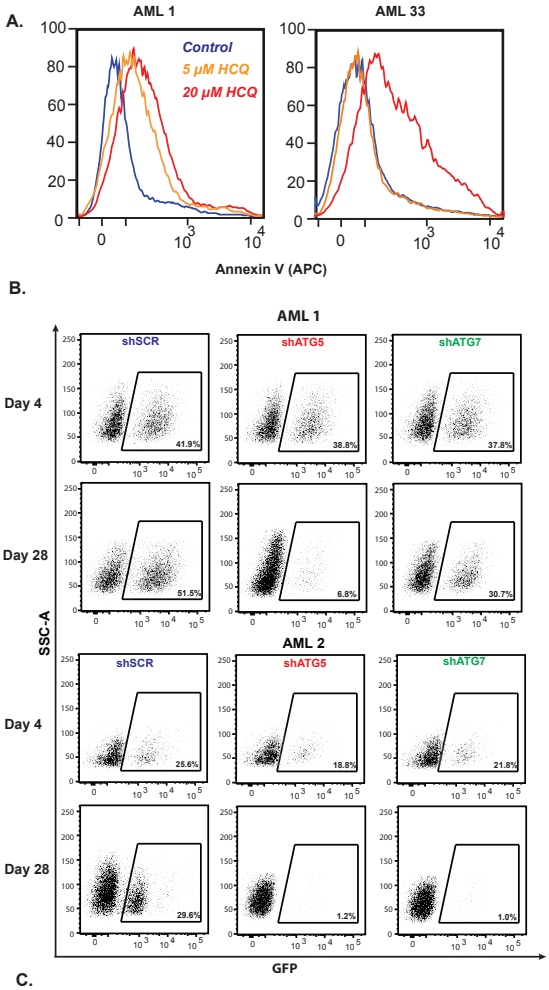

C.

	Knockdown efficiency for shATG5 and shATG7		
	shSCR	shATG5	shATG7
AML1	1,0	0,21 **	0,67 *
AML2	1,0	0,35 **	0,49 *
AML4	1,0	0,04 *	0,43 **
AML5	1,0	0,35 ***	0,50 **
AML6	1,0	0,56	0,41 *

Supplementary figure 4. Inhibition of autophagy triggers apoptosis in primary AML CD34+ cells. **(A)** Representative FACS plot showing Annexin V levels in AML CD34+ cells treated with 5 or 20 μM HCQ for 72 hours. **(B)** Representative FACS plots showing the % GFP positive cells at day 4 and day 28, for AMLs transduced with shSCR, shATG5 or shATG7-GFP. **(C)** Table showing relative expression of ATG5 or ATG7 as determined by q-PCR in shSCR, shATG5 or shATG7 transduced AMLs. RNA isolated at day 7 from FACS-sorted shSCR-GFP, shATG5-GFP or shATG7-GFP positive cells.
Error bars represent SD; *, ** or *** represents p<.05, p<0.01 or p<.001 respectively.

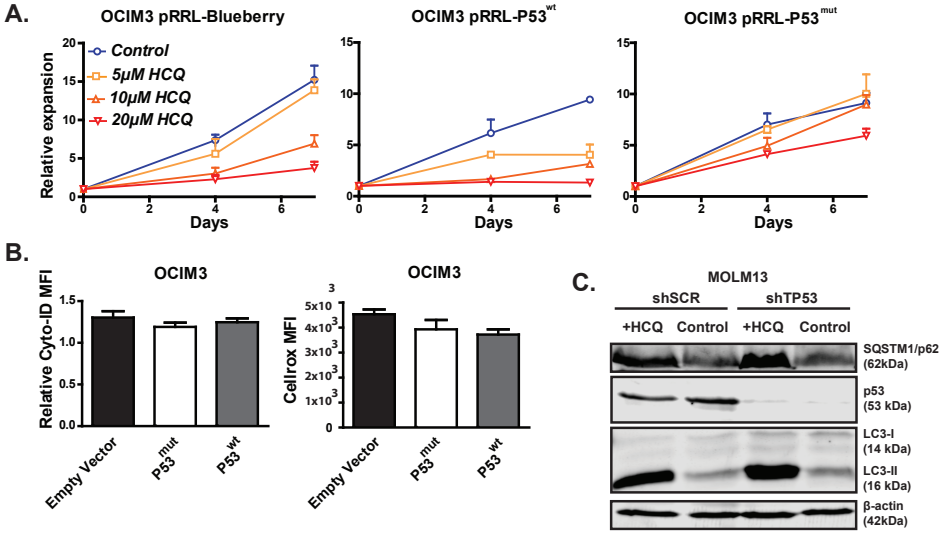

Supplementary figure 5. Inhibition of autophagy triggers a p53 dependent apoptosis response. (A) Expansion curves of OCIM3 cells transduced with pRRL-mBlueberry, pRRL-p53-mBlueberry or pRRL-p53R273H-mBlueberry cultured in the presence of different concentrations of HCQ, n=2. **(B)** OCIM3 cells transduced with pRRL-mBlueberry, pRRL-p53-mBlueberry or pRRL-p53R273H-mBlueberry, cultured for 3 days. Autophagy flux and ROS levels were subsequently determined by Cyto-ID and CellROX respectively. **(C)** Western blot showing LC3-II or p62 accumulation and p53 protein levels in MOLM13 cells transduced with shSCR or shP53 treated overnight with or without 20 μM HCQ.

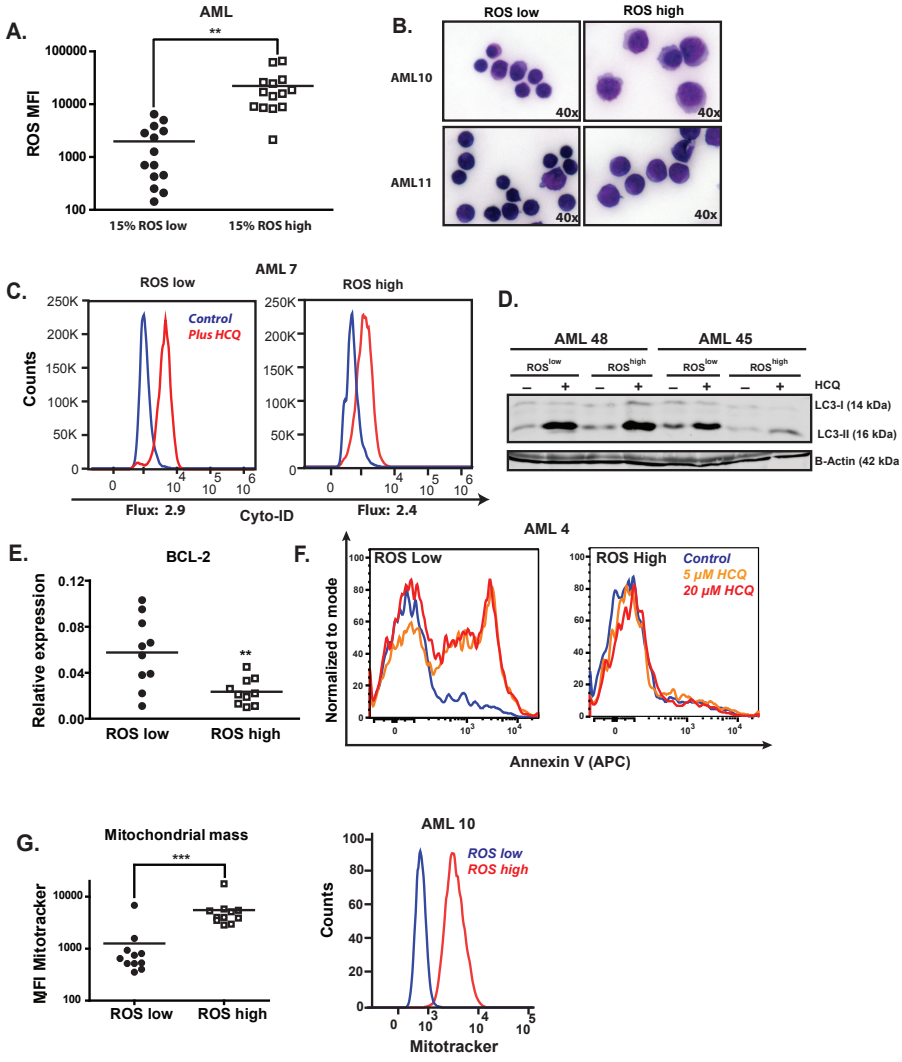

Supplementary figure 6. Autophagy is higher in the ROS low population of AML blasts. **(A)** CellROX MFI in a panel of AML CD34+ cells (N=14) and CB CD34+ (N=6). **(B)** Representative microscopy pictures of sorted AML CD34+ (n=2) ROSlow and ROShigh cells stained with May-Grünwald (MGG) (40x magnification). **(C)** Representative Cyto-ID stainings in ROSlow vs ROShigh cells treated with or without HCQ. **(D)** Facs-sorted ROSlow or ROShigh cells of two CD34+ enriched AMLs were treated overnight with HCQ and LC3-II accumulation was detected by Western blotting. β-Actin was used as loading control. **(E)** Validation of BCL-2 expression in FACS sorted ROSlow or ROShigh cells, determined by q-RT-PCR. **(F)** Representative FACS plot showing Annexin V levels in ROSlow and ROShigh AML CD34+ cells treated with different concentrations of HCQ. **(G)** Left panel: mitochondrial mass within ROSlow and ROShigh AML CD34+ cell fractions. Right panel: representative FACS plots showing MitoTracker MFI in AML ROSlow and ROShigh cells.
Error bars represent SD, ** or *** represents p<0.01 or p<.001 respectively.

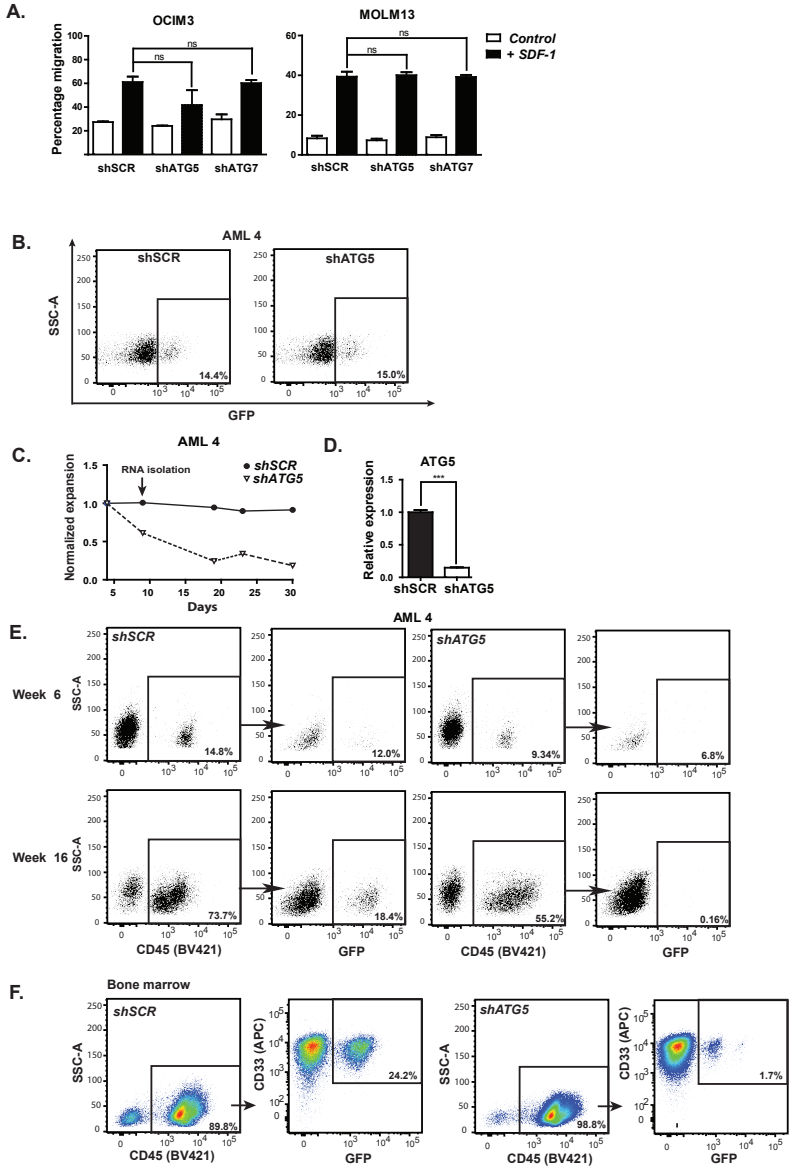

Supplementary figure 7. Knockdown of ATG5 in AML CD34+ blasts results in impaired engraftment. **(A)** GFP percentage of transduced AML CD34+ cells at the day of injection. **(B)** In vitro expansion curve of shSCR or shATG5 transduced AML CD34+ cells. **(C)** Validation of ATG5 K.D. by q-RT-PCR of in vitro expanded GFP sorted AML CD34+cells. **(D)** Day 3 after transduction, the migration towards SDF-1 of shSCR, shATG5 or shATG7 transduced OCIM3 or MOLM13 cells was evaluated in a transwell assay. **(E)** Representative FACS plots from one individual mouse within each group, showing huCD45 and GFP percentages (week 6 and 16). **(F)** Representative FACS plots showing huCD45 percentages in mice bone marrow and the GFP percentages and CD33 percentage within huCD45+ cells.

SUPPLEMENTARY TABLES

Supplementary table 1: list of cell lines with the p53 status. wt, wild type; mut, mutated.

HL60 (p53 null)	MOLM13 (p53 wt)
THP1 (p53 mut)	NB4 (p53 mut)
K562 (p53 mut)	OCIM3 (p53 wt)
KG1A (p53 mut)	

Supplementary table 2: Patient characteristics

#	Age	Male/ Female	PB/BM	$CD34^+$%	Risk	Demonstrated mutations	karyotype
1	69	M	PB	74	Adv	TP53	t(3;5),-5
2	49	F	BM	84	Fav	IDH1	Inv16
3	69	F	PB	84	Int	IDH2, FLT3-ITD	NK
4	60	M	PB/BM	39	Adv	FLT3-ITD	t(3;5)(q23;q33),+8
5	48	F	BM	30	Fav		Inv(16)
6	52	M	PB	30	Int	DNMT3A, IDH2, FLT3-ITD	NK
7	42	F	PB	42	Adv	FLT3-ITD	Complex karyotype
8	61	F	PB	61	Adv	FLT3-ITD	t(11;20)(p15;q11.2)
9	52	M	PB	52	Int	FLT3-ITD	NK
10	74	F	PB	35	Adv	TP53	Complex karyotype
11	66	F	BM	8	Int	FLT3-ITD	NK
12	71	M	BM	11	Adv	TP53	Complex karyotype
13	68	M	PB	86	Int	IDH2	+11

Abbreviations: M, male; F, female; PB, peripheral blood; BM, Bone marrow; Fav, favorable; Int, intermediate; Adv, adverse; TP53, Tumor protein P53; IDH1, isocitrate dehydrogenase 1; IDH2, Isocitrate dehydrogenase 2; FLT3-ITD, fms-like tyrosine kinase 3 internal tandem duplication; DNMT3A, DNA Cytosine-5-Methyltransferase 3 Alpha; NK, normal karyotype.

Supplementary table 3: Patient characteristics

AML Risk-group	*n*	(%) M	($\tilde{x}$)Age (range)	(%) FLT3-ITD	(%) NPM mutation	(%) TP53 mutation
Favorable	6	33	48 (28-74)	0	0	0
Intermediate	28	42	54 (17-78)	43	25	0
Adverse	17	47	62 (23-74)	29	0	35

Abbreviations: n, number of samples; , median; M, male; FLT3-ITD, fms-like tyrosine kinase 3 internal tandem duplication; NPM, nucleophosmin-1; TP53, Tumor protein P53.

Supplementary table 4: Characteristics of AML patients studied for ATG5 and ATG7 expression

AML Risk-group	*n*	(%) M	($\tilde{x}$)Age (range)
Favorable	2	0	59.5 (59-60)
Intermediate	19	47	59 (31-75)
Adverse	5	20	54 (42-68)

Abbreviations: M, male; , median.

Supplementary table 5: list of antibodies used for FACS

Antibody	Fluorochrome	Clone number	Company
Anti-CD19	BV785	HIB19	BioLegend
Anti-CD33	APC	WM-53	BioLegend
Anti-CD34	Pe-Cy7	8G12	BD Pharmingen
Anti-CD38	FITC	HIT2	BD Pharmingen
Anti-CD45	BV421	HI30	BioLegend

Supplementary table 6: list of primers used for q-RT-PCR

Gene	sequence	
LC3	Fw	5'-CGCACCTTCGAACAAAGAGTAG-3'
	Rev	5'-AGCTGCTTCTCACCCTTGTATC-3'
VMP1	Fw	5'-CAGATGAAGAGGGCACTGAAGG-3'
	Rev	5'-CTCCGATTGCTGTACCGATACC-3'
ATG10	Fw	5'-GGGAATGGAGACCATCAAAG-3'
	Rev	5'-GGTAGATGCTCCTAGATGTG-3'
BCL-2	Fw	5'-GAGGCTGGGATGCCTTTGTG-3'
	Rev	5'-GGGCCAAACTGAGCAGAGTC-3'
P53	Fw	5'-GAGATGTTCCGAGAGCTGAATGAGGC-3'
	Rev	5'-TCTTGAACATGAGTTTTTATGGCGGGAGG-3'
ATG5	Fw	5'-GGGCCATCAATCGGAAAC-3'
	Rev	5'-AGCCACAGGACGAAACAG-3'
ATG7	Fw	5'-CGTTGCCCACAGCATCATCTTC-3'
	Rev	5'-TCCCATGCCTCCTTTCTGGTTC-3'
Beclin-1	Fw	5'-CATGCAATGGTGGCTTTC-3'
	Rev	5'-TCTCCACATCCATCCTGTAG-3'
BAX	Fw	5'-CCAGCAAACTGGTGCTCAAG-3'
	Rev	5'-GGAGGCTTGAGGAGTCTCAC-3'
PUMA	Fw	5'-GACCTCAACGCACAGTACG-3'
	Rev	5'-GGCAGGAGTCCCATGATGAG-3'
PHLDA3	Fw:	5'-GGACCCTCGTGTCCTAAACC-3'
	Rev:	5'-CCTTGCCACATGGAGCACAG-3'
p21	Fw:	5'-CGACTGTGATGCGCTAATGG-3
	Rev:	5'-CGTTTTCGACCCTGAGAG-3'
RPL27	Fw	5'-TCCGGACGCAAAGCTGTCATCG-3'
	Rev	5'-TCTTGCCCATGGCAGCTGTCAC-3'
RPS11	Fw	5'-AAGATGGCGGACATTCAGAC-3'
	Rev	5'-AGCTTCTCCTTGCCAGTTTC-3'
FOXO3A	Fw	5'-ATAAGGGCGACAGCAACAG-3'
	Rev	5'-CTCTTGCCAGTTCCCTCATTC-3'
SOD1	Fw	5'-GTGCAGGGCATCATCAATTTCG-3'
	Rev	5'-AATCCATGCAGGCCTTCAGTC-3'
SOD2	Fw	5'-CCTACGTGAACAACCTGAAC-3'
	Rev	5'-AGAGCTATCTGGGCTGTAAC-3'
Catalase	Fw	5'-AGACTCCCATCGCAGTTC-3'
	Rev	5'-CCAACGAGATCCCAGTTACC-3'

Abbreviations: Rev, reverse; Fw, forward.